Theory of compressional and shear waves in fluidlike marine sediments

Michael J. Buckingham[a)]
Marine Physical Laboratory, Scripps Institution of Oceanography, University of California, San Diego, 9500 Gilman Drive, La Jolla, California 92093-0213

(Received 24 March 1997; accepted for publication 7 October 1997)

An unconsolidated, saturated marine sediment consists of a more or less loose assemblage of mineral grains in contact, with seawater in the interstices. It is postulated that the two-phase medium possesses no skeletal frame, implying that the elastic rigidity modulus of the material is zero. A theory of wave propagation in such a sediment is developed, in which the medium is treated as a fluid that supports a specific form of intergranular dissipation. Two important equations emerge from the analysis, one for compressional wave propagation and the second describing transverse disturbances. For the type of dissipation considered, which exhibits hysteresis or memory, the shear equation admits a wavelike solution, and is thus a genuine wave equation, even though the sediment shows no elastic rigidity. In effect, the medium possesses a ''dissipative'' rigidity, which is capable of supporting shear. This behavior is distinct from that of a viscous fluid, for which the shear equation is diffusionlike in character, giving rise to critically damped disturbances rather than propagating waves. The new theory predicts an attenuation coefficient for both compressional and shear waves that scales with the first power of frequency, in accord with published data. The wave theory is combined with a model of the mechanical properties of marine sediments to yield expressions relating the compressional and shear wave speeds to the grain size, the porosity, and the density of the medium. These expressions show compelling agreement with a number of measurements from the literature, representing a variety of sediment types ranging from clay to coarse sand. [S0001-4966(98)05901-3]

PACS numbers: 43.30.Ma [DLB]

LIST OF SYMBOLS

c_p	compressional wave speed (m/s)
c_s	shear wave speed (m/s)
c_0	compressional wave speed in absence of intergranular friction (m/s)
α_p	compressional attenuation coefficient (nepers/m)
α_s	shear attenuation coefficient (nepers/m)
β_p	compressional loss tangent
β_s	compressional loss tangent
Q	quality factor
χ_f	compressional dissipation coefficient
μ_c	compressional frictional rigidity modulus
μ_s	shear frictional rigidity modulus
ω	angular frequency
k_0	wave number in absence of intergranular friction
t	time
p	pressure fluctuation
$\mathbf{v}$	particle velocity
ρ	density fluctuation
$\psi(t)$	velocity potential
$\mathbf{A}(t)$	vector potential
$\Psi(j\omega)$	Fourier transform of $\psi(t)$
$h(t)$	compressional material memory function
$h_s(t)$	shear material memory function
$H(j\omega)$	Fourier transform of $h(t)$
$H_s(j\omega)$	Fourier transform of $h_s(t)$
n	compressional material memory exponent $(0<n<1)$
m	shear material memory exponent $(0<m<1)$
u_g	mean grain diameter, microns
N	porosity $(0<N<1)$
ρ_0	bulk density of sediment (kg/m^3)
κ	bulk modulus of sediment (Pa)
γ	volume ratio of smaller to larger grains in a bimodal sediment
$\rho_w=1024$ kg/m^3	density of pore water
$\rho_g=2700$ kg/m^3	density of mineral grains
$\kappa_w=2.25\times10^9$ Pa	bulk modulus of pore water
$\kappa_g=1.47\times10^{10}$ Pa	bulk modulus of mineral grains
$\Delta=3$ μm	rms particle roughness
$P=0.63$	packing factor of randomly packed smooth spheres
$u_0=1000$ μm	reference grain diameter
$\mu_0=2\times10^9$ Pa	compressional frictional rigidity constant
$\mu_1=5.1\times10^7$ Pa	shear frictional rigidity constant

[a)]Also affiliated to: Institute of Sound and Vibration Research, The University, Southampton SO17 1BJ, England.

INTRODUCTION

A theory of the acoustic and mechanical properties of unconsolidated marine sediments was recently introduced and developed in a paper by Buckingham,[1] hereafter referred to as I. Central to the theory is a specific form of intergranular dissipation, which exhibits an unusual form of hysteresis. It is shown in I that this particular type of dissipation gives rise to many of the observed properties of saturated sands and silts. The sediment was treated in I as an equivalent fluid in which shear-wave propagation was neglected.

Actual sediments have long been known to support shear waves,[2–4] although the shear speed is low compared with the compressional speed. For instance, a medium-to-coarse sand with a grain diameter of 500 μm has a compressional wave speed in the region of 1750 m/s, whereas the shear speed is of the order of 100 m/s.[5] In finer sediments the shear speed is even lower. Typically, the ratio of compressional speed to shear speed is somewhat greater than 10 in saturated sediments,[6] but is less than 2 for water-saturated rocks,[7] suggesting that the geoacoustic properties of consolidated rocks and unconsolidated sediments may be governed by different physical mechanisms.

In a series of classic papers, Biot[8–11] developed a theory of acoustic propagation in fluid-saturated porous media. The materials he considered consist of a solid elastic matrix, or skeletal frame, containing a compressible, viscous fluid. An example of such a medium is water-saturated rock. Biot's viscoelastic theory leads to the prediction of three types of body wave, of which two are longitudinal (compressional) and one is transverse (shear). The compressional wave of the first kind, or fast wave, shows relatively little attenuation and corresponds to displacements of the frame and the interstitial fluid which are in phase. Out of phase displacements give rise to the compressional wave of the second kind, the slow wave, which suffers relatively high attenuation.

Observations of fast, slow, and shear waves have been reported in a porous medium consisting of fused glass beads immersed in water.[12,13] Such a material resembles rock in that the fused beads formed a consolidated, elastic skeletal frame. This is the type of medium addressed by the Biot theory, and it was found that all the measured wave speeds (2.81, 0.96, and 1.41 km/s for the fast, slow, and shear waves, respectively) conformed with the predictions of the theory.

In a second experiment by the same researchers,[13] a minor change in the microgeometry lead to a radical change in the acoustic behaviour of the porous medium. Instead of being fused, the beads were left loose, or unconsolidated, much like a sediment consisting of mineral grains and seawater. A fast wave with a speed of 1.79 km/s was observed, comparable with that of the compressional wave in sediments, but neither a slow wave nor a shear wave were detected. The absence of a shear wave was attributed to scattering of the short, ultrasonic shear wavelengths used in the experiment.

As with the compressional-to-shear speed ratio, the fundamentally distinct behavior of the fused and loose glass beads suggests that different physical processes may be at work in consolidated and unconsolidated materials. In this article, we shall identify the terms ''consolidated'' and ''unconsolidated'' with the presence and absence, respectively, of a skeletal frame. In a consolidated medium like rock, the porous mineral structure constitutes the elastic, skeletal frame, and the Biot theory or an appropriate modification of it is expected to hold. By way of contrast, the mineral grains in an unconsolidated sediment are, on a microscopic scale, mobile with respect to one another, suggesting that the material possesses no skeletal frame. In this case, the mechanism of intergranular friction introduced in I is presumed to govern the acoustic properties of the medium. The absence of a frame eliminates the possibility of a slow wave in an unconsolidated material.

If it is accepted that an unconsolidated marine sediment does not possess a skeletal frame, the medium cannot be regarded as an elastic solid. In fact, in several ways a saturated sediment is fluidlike in character. We postulate here that the sediment acts as a true fluid, in the sense that its dynamic rigidity or elastic shear modulus is identically zero. This would seem to suggest that the sediment is incapable of supporting shear waves, in contradiction with observations in the laboratory and *in situ*, but this is not so.

There is no doubt that a saturated sediment exhibits an ''effective rigidity,'' allowing the medium to support the transmission of transverse waves. It is demonstrated here that the rigidity may arise from a certain type of dissipation at intergrain contacts. In other words, internal dissipation (not elasticity) in the fluid medium is responsible for shear wave propagation. This is a fairly radical statement, since it is easily proved that a conventional fluid, in which the dissipation is due to viscosity, cannot support transverse waves.[14] It turns out, however, that if the internal dissipation exhibits an appropriate form of memory, a degree of stiffness or rigidity is introduced into the medium, which allows shear waves to propagate.

The properties of a particular type of fluid that is capable of supporting shear waves and is also representative of unconsolidated marine sediments, are developed in this article. The basic theoretical ideas in I are extended to include the effects of shear arising from intergranular dissipation. By adapting a standard argument, separated wave equations are established for the compressional and shear waves in a sediment whose rigidity arises, not from frame elasticity, but from the dissipative force between contiguous mineral particles. As in I, the dissipation term in each wave equation is formulated as a temporal convolution between a material memory function and the particle velocity. The inclusion of the shear wave has no effect on the properties of the compressional wave, which remain exactly as described in I. Both the compressional and the shear wave emerging from the new theory show characteristics that are in accord with available experimental data. In particular, the attenuation coefficient of both waves is accurately proportional to the first power of frequency, consistent with the observations of Hamilton,[15,16] Brunson,[17,18] and others.

I. BASIC FORMULATION

To derive the wave equations for compressional and shear waves in an unconsolidated sediment, we assume that the material is macroscopically homogeneous, isotropic, time

invariant, and infinite. In effect, the granular medium is treated as a dissipative (but not viscous), compressible fluid, with an elastic rigidity modulus of zero. The absence of elastic rigidity means that the material is not a Hookean solid, even though it will be shown to support transverse waves.

To begin, consider first the (fictitious) case when dissipation is entirely absent, that is, the medium is simply a lossless, compressible fluid. Then the equation of motion is

$$\rho_0 \frac{\partial \mathbf{v}}{\partial t} + \text{grad } p = 0, \tag{1}$$

where $\mathbf{v}$ is particle velocity, ρ_0 is bulk density, and p is the pressure fluctuation. From conservation of mass and the equation of state,

$$\frac{\partial p}{\partial t} + \kappa \text{ div } \mathbf{v} = 0, \tag{2}$$

where κ is the bulk modulus of the medium, and, on combining Eqs. (1) and (2), the familiar wave equation for compressional waves in the medium is obtained:

$$\rho_0 \frac{\partial^2 \mathbf{v}}{\partial t^2} = \kappa \text{ grad div } \mathbf{v}. \tag{3}$$

There is no solution of this equation that corresponds to transverse waves. The speed of sound (i.e., the phase speed of the compressional wave) in the lossless fluid, c_0, follows from Eq. (3):

$$c_0 = \sqrt{\frac{\kappa}{\rho_0}}. \tag{4}$$

An expression for c_0 in terms of the bulk moduli and densities of the two constituents of the lossless sediment, mineral grains and seawater, will be given later.

Now suppose that the medium is allowed to support intergranular dissipation. Following the spirit of I, Eq. (3) must be modified by adding to the right-hand side two dissipation terms [see, for example, the analogous Navier–Stokes equation (2.3.18) for viscous dissipation, p. 162 in Morse and Feshbach[14]]. Thus the equation appropriate to a saturated sediment is proposed as

$$\rho_0 \frac{\partial^2 \mathbf{v}}{\partial t^2} = \kappa \text{ grad div } \mathbf{v} + \left(\frac{4}{3} \eta_f + \lambda_f \right) \text{grad div } \frac{\partial}{\partial t} [h(t) \otimes \mathbf{v}(t)] - \eta_f \text{ curl curl } \frac{\partial}{\partial t} [h_s(t) \otimes \mathbf{v}(t)], \tag{5}$$

where $h(t)$ and $h_s(t)$ are, respectively, material ''memory'' functions for compressional and shear disturbances, and the symbol $\otimes$ denotes a temporal convolution. The basis of the dissipation terms in Eq. (5) is that the components of the frictional stress tensor involve the appropriate memory function convoluted with the particle velocity, rather than the velocity itself.

If $h(t)$ and $h_S(t)$ were delta functions, Eq. (5) would reduce identically to the form appropriate to a viscous fluid,[19,20] since $\delta(t) \otimes \mathbf{v}(t) = \mathbf{v}(t)$. Thus viscosity corresponds to the situation where the medium has no memory, that is, previous events have no effect on the current response. However, with other forms for the memory functions, representing the influence of earlier states on present behaviour, the dissipation may be radically different in character from viscosity. A specific form for $h(t)$ was introduced in I as being representative of dissipation in marine sediments.

Although the dissipation coefficients η_f and λ_f in Eq. (5) are analogous, respectively, to the shear and bulk viscosities of a fluid, the subscript f highlights the fact that these coefficients are actually associated with intergranular friction, not with viscosity. It is important to notice that there is no term in Eq. (5) of the form μ curl curl $\mathbf{v}$, which would necessarily be present to represent the effects of rigidity if the medium were elastic with rigidity modulus μ. The absence of such a term is consistent with our hypothesis that a marine sediment has no elastic rigidity, that is, the rigidity modulus, μ, is strictly zero. If the dissipation mechanism were viscosity, the absence of the rigidity term in Eq. (5) would lead to a diffusion type of equation for the vector potential of the field, implying that the shear disturbance would not be a true wave but would decay in time and space. In other words, a viscous fluid does not support shear waves. However, as shown below, with an appropriate choice of the memory function $h_s(t)$, a wavelike solution of Eq. (5) for transverse disturbances is admissible and shear wave transmission is possible as a direct result of the intergranular dissipation.

The functions $h(t)$ and $h_s(t)$, representing, respectively, the material memory functions for the compressional and shear waves, are assigned the forms

$$h(t) = u(t) \frac{t_0^{n-1}}{t^n}, \quad 0 < n \ll 1 \tag{6}$$

and

$$h_s(t) = u(t) \frac{t_1^{m-1}}{t^m}, \quad 0 < m \ll 1, \tag{7}$$

where the presence of $u(t)$, the unit step function, ensures that the medium is causal. This type of memory function has been discussed at length in I. It is shown below that the small exponents n and m, respectively, control the attenuation of the compressional and shear wave, but have only a very minor dispersive effect on the wave speeds. The temporal coefficients t_0 and t_1 appear in Eqs. (6) and (7) to maintain the correct units of inverse time for the memory functions, that is, the convolutions have the dimensions of velocity.

Equation (5) in conjunction with Eqs. (6) and (7) is the fundamental equation governing the propagation of compressional and shear waves in the dissipative fluid sediment.

II. WAVE EQUATIONS

According to Helmholtz's theorem,[14] any vector field, $\mathbf{v}$, may be expressed as the sum of the gradient of a scalar potential, ψ, and the curl of a zero-divergence vector potential $\mathbf{A}$:

$$\mathbf{v} = \text{grad } \psi + \text{curl } \mathbf{A}; \quad \text{div } \mathbf{A} = 0. \tag{8}$$

Following a standard form of analysis,[21] the first of the expressions in Eq. (8) is substituted into Eq. (5), which may

then be separated into two equations by equating terms in ψ and $\mathbf{A}$:

$$\nabla^2\psi - \frac{1}{c_0^2}\frac{\partial^2\psi}{\partial t^2} + \frac{(\frac{4}{3}\eta_f + \lambda_f)}{\rho_0 c_0^2}\frac{\partial}{\partial t}\nabla^2[h(t)\otimes\psi(t)] = 0 \quad (9)$$

and

$$\frac{\eta_f}{\rho_0}\frac{\partial}{\partial t}\nabla^2[h_s(t)\otimes\mathbf{A}(t)] - \frac{\partial^2\mathbf{A}}{\partial t^2} = 0, \quad (10)$$

where ∇^2 is the Laplacian. The identities curl grad $\psi = 0$, div curl $\mathbf{A} = 0$, and curl curl $\mathbf{A} = -\nabla^2\mathbf{A}$ were used in deriving these expressions. The wave equation for compressional waves [Eq. (9)] formed the basis of the discussion in I.

For a shear wave of vertical polarization, the vector potential can be chosen so that only one component differs from zero. Setting

$$\mathbf{A} = -\frac{\partial\psi_s}{\partial r}\mathbf{e}_\phi, \quad (11)$$

where r is horizontal range, $\mathbf{e}_\phi$ is the unit vector normal to the plane of propagation and ψ_s is a scalar shear potential, Eq. (10) reduces to

$$\frac{\eta_f}{\rho_0}\nabla^2[h_s(t)\otimes\psi_s(t)] - \frac{\partial\psi_s}{\partial t} = 0. \quad (12)$$

This is a new equation for transverse disturbances, which is discussed below.

Although it may look diffusionlike in character, Eq. (12) together with the expression for $h_s(t)$ in Eq. (7) admits a wavelike solution and hence may be regarded as a genuine wave equation. It is easy to see, however, that if $h_s(t)$ were a delta function, corresponding to viscous dissipation, Eq. (12) would indeed take the form of a diffusion equation, whose only solution is a critically damped disturbance, which is not a true wave. This, of course, is why a viscous fluid cannot support transverse waves. Clearly, Eq. (12) is an important result: while being consistent with the special case of a viscous fluid, it allows for the possibility that certain types of dissipative fluids (i.e., media whose elastic rigidity modulus is zero) are capable of supporting propagating shear waves.

The wave equations in Eqs. (9) and (12) are expressed in the time domain, and the coefficients appearing in them are real constants representing the mechanical properties of the medium. Thus these constants are not permitted to become complex, nor may they show any frequency dependence.

When the compressional and shear-wave equations are Fourier transformed with respect to time they become

$$\nabla^2\Psi + \frac{\omega^2}{c_0^2}\Psi + j\omega\frac{(\frac{4}{3}\eta_f + \lambda_f)}{\rho_0 c_0^2}H(j\omega)\nabla^2\Psi = 0 \quad (13)$$

and

$$\frac{\eta_f}{\rho_0}H_s(j\omega)\nabla^2\Psi_s - j\omega\Psi_s = 0, \quad (14)$$

where ω is angular frequency, (Ψ, Ψ_s) are the Fourier transforms of the compressional and shear waves (ψ, ψ_s), and similarly (H, H_s) are the transforms of the memory functions (h, h_s). Now the Fourier transform of the memory functions in Eqs. (6) and (7) is a standard form:[22]

$$H(j\omega) = \frac{\Gamma(1-n)}{(j\omega t_0)^{1-n}} \quad (15)$$

and

$$H_s(j\omega) = \frac{\Gamma(1-m)}{(j\omega t_1)^{1-m}}, \quad (16)$$

where $\Gamma(..)$ is the gamma function, which is essentially unity since n and m are very small numbers. On substituting these expressions into Eqs. (13) and (14), we arrive at the following reduced wave equations for the compressional and shear waves:

$$[1 + (j\omega t_0)^n\chi_f]\nabla^2\Psi + \frac{\omega^2}{c_0^2}\Psi = 0 \quad (17)$$

and

$$\frac{\mu_s}{\rho_0}\nabla^2\Psi_s + \frac{\omega^2}{(j\omega t_1)^m}\Psi_s = 0. \quad (18)$$

As in I, the dimensionless dissipation coefficient χ_f appearing in Eq. (17) is simply an amalgamation of several parameters:

$$\chi_f = \frac{(\frac{4}{3}\eta_f + \lambda_f)\Gamma(1-n)}{\rho_0 c_0^2 t_0} = \frac{\mu_c}{\rho_0 c_0^2}, \quad (19)$$

where μ_c may be regarded as the compressional, dissipative rigidity modulus. The coefficient χ_f governs the properties of the compressional wave, that is to say, the wave speed and attenuation. The new coefficient, μ_s, appearing in the reduced shear wave equation [Eq. (18)] is

$$\mu_s = \frac{\eta_f}{t_1}\Gamma(1-m). \quad (20)$$

The importance of this coefficient should be recognized, since it is the transverse ''effective rigidity modulus'' of the sediment, arising directly from the intergranular dissipation. It is because of the nonzero value of μ_s that shear waves can propagate in the fluidlike sediment. Notice that, like the rigidity modulus of an elastic solid, μ_c and μ_s have the dimensions of pressure, but neither is an elastic modulus: Both scale with the level of the intergranular dissipation, and hence are direct measures of the dissipative rigidity of the medium.

III. WAVE SPEED AND ATTENUATION

Consider one-dimensional, plane-wave propagation in the x direction. For this simple situation, the reduced wave equation for the compressional wave [Eq. (17)] can be written as

$$\frac{\partial^2\Psi}{\partial x^2} + \frac{\omega^2}{c_0^2[1 + (j\omega t_0)^n\chi_f]}\Psi = 0 \quad (21)$$

and similarly for the shear wave [Eq. (18)],

$$\frac{\partial^2 \Psi_s}{\partial x^2} + \frac{\omega^2}{(j\omega t_1)^m(\mu_s/\rho_0)}\,\Psi_s = 0. \tag{22}$$

By inspection, the solutions of these equations are

$$\Psi = \Psi_0 \exp - j\frac{\omega}{c_0\sqrt{1+(j\omega t_0)^n\chi_f}}\,|x| \tag{23}$$

and

$$\Psi_s = \Psi_{s0} \exp - j\,\frac{\omega}{\sqrt{(j\omega t_1)^m(\mu_s/\rho_0)}}\,|x|, \tag{24}$$

where Ψ_0 and Ψ_{s0} are the amplitudes of the compressional and shear wave, respectively. Both of these expressions represent a propagating, exponentially damped wave, that is, the dissipative fluid described by Eqs. (17) and (18) supports not only a compressional wave but also a well-behaved shear wave.

Following I, accurate approximations for the wave speeds and attenuations may be developed on the basis of a straightforward argument. To first order in the small parameter n, the following expressions are valid:

$$[\mathrm{sgn}(\omega)j]^n = \cos(n\pi/2) + j\ \mathrm{sgn}(\omega)\ \sin(n\pi/2)$$
$$\approx 1 + (jn\pi/2)\mathrm{sgn}(\omega), \tag{25}$$

and

$$(|\omega|t_0)^n = \exp[n\ \ln(|\omega|t_0)] = 1 + n\ \ln(|\omega|t_0) + \cdots . \tag{26}$$

Obviously, similar expressions hold for the term raised to the power of m in Eq. (24). The signum function in Eq. (25) has been included to accommodate negative frequencies. Hence, to the same order of approximation, the compressional and shear-wave speeds, c_p and c_s, respectively, can be written as

$$c_p = c_0\ \mathrm{Re}\sqrt{1+(j\omega t_0)^n\chi_f}$$
$$= c_0\sqrt{1+\chi_f}\left[1 + \frac{n\chi_f}{2(1+\chi_f)}\ \ln(|\omega|t_0)\right] \tag{27}$$

and

$$c_s = \mathrm{Re}\sqrt{(j\omega t_1)^m(\mu_f/\rho_0)}$$
$$= \sqrt{\frac{\mu_s}{\rho_0}}\left[1 + \frac{m}{2}\ \ln(|\omega|t_1)\right]. \tag{28}$$

According to these expressions, both wave speeds show very weak logarithmic dispersion, which in most circumstances is entirely negligible (see I). Thus the wave speeds are essentially given by the frequency-independent expressions

$$c_p = c_0\sqrt{1+\chi_f} \tag{29}$$

and

$$c_s = \sqrt{\frac{\mu_s}{\rho_0}}. \tag{30}$$

It is interesting that the shear speed takes exactly the same form as it would in an elastic solid, except that the dynamic rigidity modulus, μ, has been replaced by the dissipative rigidity modulus, μ_s. Since μ_s scales with the level of dissipation [Eq. (20)], it is clear that the shear speed goes to zero as the losses vanish, consistent with observations in actual marine sediments.[3,23,24]

To first order in n and m, the compressional and shear attenuation coefficients, α_p and α_s, respectively, from Eqs. (23)–(26), are

$$\alpha_p = \beta_p\,\frac{|\omega|}{c_p} = \frac{n\pi\chi_f}{4(1+\chi_f)}\,\frac{|\omega|}{c_p}, \tag{31}$$

and

$$\alpha_s = \beta_s\,\frac{|\omega|}{c_s} = \frac{m\pi}{4}\,\frac{|\omega|}{c_s}. \tag{32}$$

The dimensionless, frequency-independent loss tangents β_p and β_s, representing the imaginary part of the complex wave number relative to the real part, are defined by these expressions. Notice that both attenuation coefficients, α_p and α_s, scale as the first power of frequency. Moreover, the weak dispersion expressed in Eqs. (27) and (28) is exactly as required by the Kronig–Kramers relationships[25,26] for a medium with attenuation of the form given in Eqs. (31) and (32), irrespective of the details of the mechanism responsible for the dissipation.[27] The linear scaling of attenuation with frequency emerges from the new theory quite naturally. It has been discussed at length in I in connection with attenuation of the compressional wave, for which extensive supporting data are available.[15,16] Far fewer measurements have been made on the attenuation of shear waves in unconsolidated marine sediments, but the little evidence that has been published is consistent with Eq. (32).

IV. SHEAR ATTENUATION VERSUS FREQUENCY MEASUREMENTS

Figure 1 shows the attenuation of shear waves as a function of frequency in water-saturated medium sand, as measured in the laboratory by Brunson and Johnson[17] and Brunson.[18] The data points in the figure show the values tabulated by these authors. All three sand samples represented in the figure had approximately the same mean grain diameter, lying between 350 and 380 μm. The solid lines in the figure are least-squares, power-law fits to the data, and the exponent of each is shown in the corresponding panel. These exponents are all very close to unity, consistent with the linear frequency dependence for the attenuation expressed in Eq. (32). No shear speed was reported for the laboratory sediments, but if for the moment it is assumed to be $c_s = 120$ m/s, then from Eq. (32) the value of m is found to be $m \approx 0.049$, which is comparable to the values of n found for compressional waves in I.

In addition to his sand data, Brunson[18] also reported measurements of shear attenuation in a granular medium consisting of loose, spherical, quartz glass beads immersed in water. The beads were sorted, with a mean diameter of 380 μm, that is, much the same as the sands in Fig. 1. Figure 2 shows the results of the measurements, as tabulated by Brunson, and also a power-law, least-squares fit to the data. The linear relationship between attenuation and frequency exhibited by this particular medium is quite striking, and, as with the sand data in Fig. 1, is in excellent agreement with

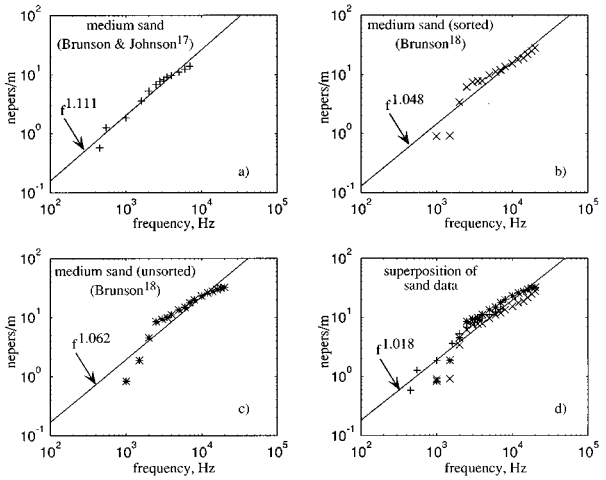

FIG. 1. Shear-wave attenuation, α_s, versus frequency, f, in saturated medium sands with mean grain diameters between 350 and 380 μm. The symbols represent laboratory data as follows: (a) saturated angular sand, from Brunson and Johnson (Ref. 17), Table II; (b) sorted sand, from Brunson (Ref. 18), Table 2; (c) unsorted sand, from Brunson (Ref. 18), Table 2; and (d) superposition of the data in panels (a)–(c). The solid lines are least-squares fits to the data of the power law $\alpha_s = af^b$, where f is frequency and a, b are constants.

Eq. (32). Assuming the same shear speed of 120 m/s, the value of the exponent m for the glass beads is $m \approx 0.025$, which is about half that found for the sand.

Although the data sets in Figs. 1 and 2 represent a very limited sample, the trend that they follow is consistent with the linear frequency dependence expressed by Eq. (32). Curiously, in assessing his own shear-attenuation experiments on sands and glass beads, Brunson[18] made the following statement. ''None of the three sediments exhibited a truly linear frequency dependence across the entire frequency range, although linear regression fits to the data produced reasonable results, particularly for the ''ideal'' spherical beads.'' This conveys the impression that the shear attenuations measured by Brunson do not scale as the first power of frequency. Such an interpretation is difficult to reconcile with the plots shown in Figs. 1 and 2.

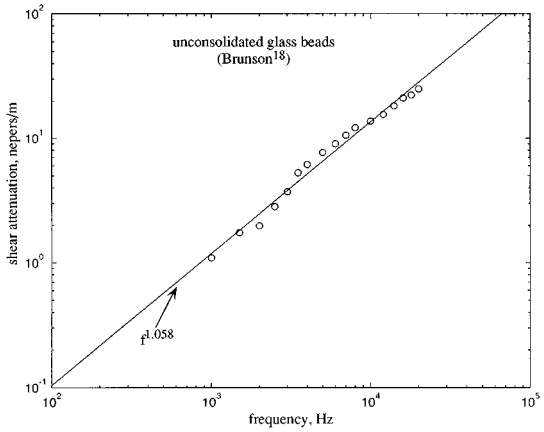

FIG. 2. Shear-wave attenuation, α_s, versus frequency, f, in water-saturated, unconsolidated glass beads. The symbols represent data from Brunson (Ref. 18), Table 2, and the solid line is a least-squares fit to the data of the power law $\alpha_s = af^b$, where a, b are constants.

From a theoretical point of view, the question of whether the attenuation (compressional and shear) in sediments is proportional to frequency is extremely important. Attenuation measurements, especially for shear, are difficult to make and invariably the data points will show some random scatter, especially at lower frequencies, where the wavelength becomes comparable to the dimensions of the experimental set up. There is some evidence of such scatter in Brunson's sand data shown in Fig. 1(a), (b), and (c). However, the only feature common to all three data sets in Fig. 1 is their near-linear dependence on frequency. The detailed excursions of the data points about the regression lines show no obvious systematic behavior, suggesting that the fine structure in the data bears little relation to the primary physical mechanism responsible for the attenuation in these materials. Accordingly, the only reasonable interpretation of Brunson's data[17,18] for sands, and also of course for the glass beads, is that the principal dependence exhibited by the shear attenuation is a near-linear scaling with frequency.

V. WOOD'S EQUATION FOR c_0

The parameter c_0 defined in Eq. (4) is a constant for a given sediment, since it depends only on the bulk modulus and the density of the medium. It is the value that the compressional wave speed would have in the absence of inter-granular losses, that is, if there were no dissipative rigidity. The effect of the rigidity is to increase the stiffness of the medium, which in turn raises the compressional speed, c_p, above the value c_0. This physical interpretation of c_0 and c_p is consistent with Eqs. (3) and (5), and also with the expression for c_p in Eq. (29).

In the absence of inter-granular dissipation, the material would be a simple, lossless, two-phase medium, consisting of mineral grains and seawater. The sound speed, c_0, in such a medium is given by Wood's equation,[28] in terms of weighted means of the bulk moduli and the densities of the constituent materials. An interesting aspect of Wood's equation is that, over the years, it has been discussed by several authors in connection with marine sediments, but always in the context of the observable compressional wave speed, c_p, rather than the nonobservable speed, c_0. Although Wood's equation alone does not yield c_p, since it takes no account of rigidity in the material, it is developed below to provide an expression for c_0, which will be used later when evaluating the actual wave speed, c_p, in Eq. (29).

To express c_0 in terms of the densities and bulk moduli of the mineral grains and seawater, the density of the sediment is written as

$$\rho_0 = N\rho_w + (1-N)\rho_g, \tag{33}$$

where N is the porosity of the material, $\rho_w = 1024$ kg/m^3 is the density of seawater, and $\rho_g = 2700$ kg/m^3 is the density of quartz sand grains. Similarly, the bulk modulus of the medium, κ, is given by

$$\frac{1}{\kappa} = N\,\frac{1}{\kappa_w} + (1-N)\,\frac{1}{\kappa_g}, \tag{34}$$

where $\kappa_w = 2.25 \times 10^9$ Pa is the bulk modulus of the interstitial seawater. As in I, the bulk modulus of the mineral grains is taken to be $\kappa_g = 1.47 \times 10^{10}$ Pa, which is the geometric mean of the values reported by Chotiros[29,30] (6×10^9 Pa) and Stoll[31] (3.6×10^{10} Pa). From the definition in Eq. (4), the sound speed in the absence of friction can now be written as

$$c_0 = \sqrt{\frac{\kappa_w \kappa_g}{[N\rho_w + (1-N)\rho_g][N\kappa_g + (1-N)\kappa_w]}}, \tag{35}$$

which is Wood's equation for c_0.

The porosity, N, in Eq. (35) is related to the mean diameter, u_g, of the mineral grains comprising the sediment. To establish the relationship between N and u_g, a packing argument must be invoked. Such a relationship, in conjunction with Eq. (35), will allow c_0 to be evaluated for various types of sediment, as characterized by the grain size.

VI. COUPLING OF WAVE PROPERTIES AND MECHANICAL PARAMETERS

A simple packing model of a saturated sediment was introduced in I, in which the roughness of the mineral particles plays an important role. The sediment was assumed to consist of randomly packed, rough spheres, which gave rise to the following expression for the porosity as a function of grain size:

$$N = 1 - P\left\{\frac{u_g + 2\Delta}{u_g + 4\Delta}\right\}^3, \tag{36}$$

where $P = 0.63$ is the packing factor for a random arrangement of smooth spheres.[32] In Eq. (36), the mean particle diameter, u_g, is measured in microns, and Δ is the rms roughness measured about the mean surface of a particle. A value of $\Delta = 3$ μm, independent of particle size, is appropriate for surficial sediments but may need modification for deeper sediments, where the overburden pressure could reduce the porosity by squeezing the particles closer together.

According to Eq. (36), the porosity of a very coarse-grained sediment having a mean grain size much greater than the roughness scale is $N_{\min} = 1 - P = 0.37$, whereas the very finest-grained material, in which u_g is vanishingly small, shows a porosity $N_{\max} = 1 - (P/8) = 0.92$. In between these two extreme values, the porosity expressed by Eq. (36) decays monotonically with increasing grain size, as shown in Fig. 3. The measured porosity of many marine sediments is in accord with Eq. (36), as can be seen in Fig. 3(a), where the symbols represent data from Hamilton[15,33] and Richardson and Briggs.[24] Note that the data span almost three decades of grain size, corresponding to sediment types ranging from the finest-grained clays to coarse sand. At either end of this range, the data approach the values $N_{\min} = 0.37$ and $N_{\max} = 0.92$, as predicted by Eq. (36), and elsewhere the measurements fall nicely on the theoretical curve. Similar agreement is found between the theoretical density determined from Eqs. (33) and (36) and Hamilton's[15,33] measurements of density versus grain size, as shown in Fig. 4(a).

However, not all sediments are described by Eq. (36), as illustrated in Fig. 3(b), which is the same as Fig. 3(a) except

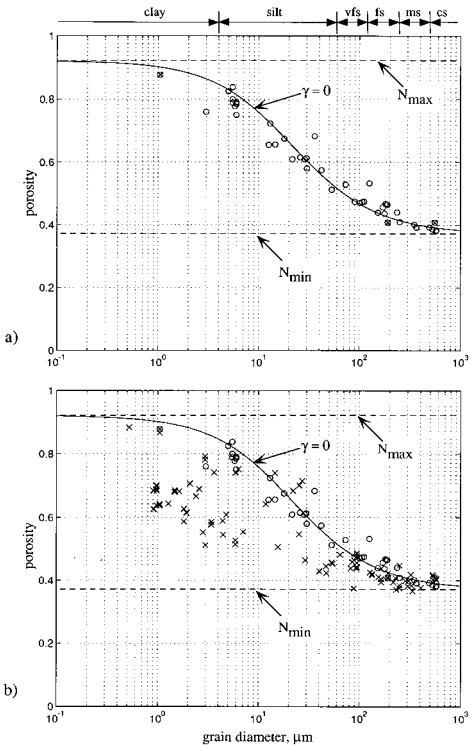

FIG. 3. Porosity versus grain size. In (a) and (b) the solid line is the theoretical expression in Eq. (36) and the symbols represent data from the following sources: (a) and (b) open circle (○), Hamilton (Refs. 15, 33); (a) and (b) circle with cross (⊗), Richardson and Briggs (Ref. 24); (b) cross (×), Richardson *et al.* (Refs. 23, 34–38). The key to the sediment types is: cs=coarse sand; ms=medium sand; fs=fine sand; vfs=very fine sand.

that it includes several additional data sets from Richardson and colleagues.[23,34–38] It is evident that the porosity exhibited by some of the finer sediments, the silts and clays, is not a single-valued function of the particle size, and that many of the data points for these materials fall below the theoretical curve [Eq. (36)]. The corresponding densities are higher than predicted by Eqs. (33) and (36), as shown in Fig. 4(b), which is the same as Fig. 4(a) but with the addition of data from Richardson *et al.*[23,36,37] Incidentally, most of Richardson's density data are not determined directly as a mass-to-volume ratio but are computed from the measured porosity using the weighted mean of the two-phase medium in Eq. (33). Thus the data represented by the crosses (x) in Figs. 3(b) and 4(b) are not independent, making it inevitable that low porosities will appear as high densities.

Several factors could be responsible for the reduced porosity in silts and clays. As discussed in I, one possibility is the presence of a secondary, smaller particle species, which in-fills the pores spaces, thus displacing water and reducing the porosity of the medium. To accommodate a bimodal grain-size distribution, the expression in Eq. (36) must be modified as follows:

$$N = 1 - P\left\{\frac{u_g + 2\Delta}{u_g + 4\Delta}\right\}^3 (1 + \gamma), \tag{36'}$$

where γ is the volume ratio of the primary particle species to the smaller, in-filling particles. In the case of the coarser

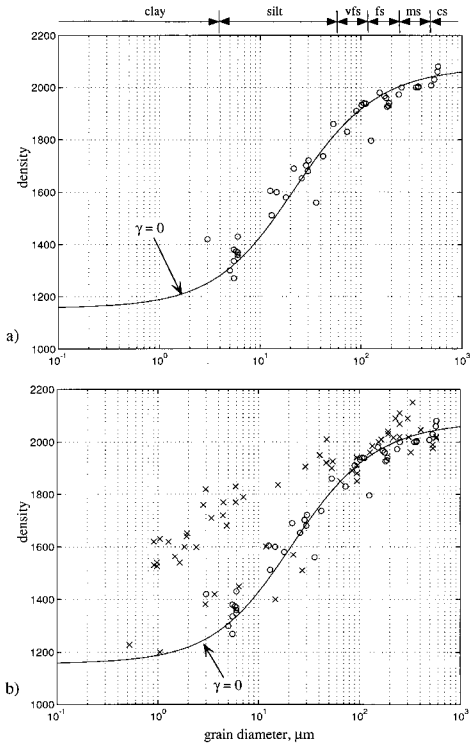

FIG. 4. Density versus grain size. In (a) and (b) the solid line is the theory from Eqs. (33) and (36), and the symbols represent data from the following sources: (a) and (b) open circle (○), Hamilton (Refs. 15, 33); (b) cross (×), Richardson *et al.* (Refs. 23, 36, 37). The key to the sediment types is in the legend to Fig. 3.

sediments, the sands and many of the coarser silts, which tend to show a unimodal grain-size distribution, the value of γ may be safely set to zero, but, for the finer sedimentary materials with an admixture of clay, it is important to identify the appropriate value of γ. Sometimes γ is reported indirectly, for example, as a percentage clay in silt. Otherwise, γ could be evaluated by matching Eq. (36′) to a direct measurement of porosity.

The sound speed, c_0, in the absence of friction varies with the mean grain size, u_g, as given by Eqs. (35) and (36′). In order to go one step further and express the compressional speed c_p [Eq. (29)] and shear-wave speed c_s [Eq. (30)] in terms of the grain size, the compressional and shear dissipation coefficients, μ_c and μ_s, respectively, must be expressed as functions of u_g. To help establish the required relationships, the Hertz theory of deformation of two spherical, elastic bodies in contact[39] is used as a guide.

According to the Hertz theory, when two identical elastic spheres are pressed together by a force F, a circular area of contact forms between them whose radius, a, is given by the cube-root expression

$$a=\sqrt[3]{\frac{3}{4}\frac{F(1-\sigma^2)}{E}R}, \tag{37}$$

where R is the sphere radius and (E,σ) are, respectively, Young's modulus and Poisson's ratio of the material constituting the spheres. The maximum tensile stress occurs around the circumference, $2\pi a$, of the area of contact, and acts in the radial direction. In the present context, the two spheres, of course, are being considered as adjacent mineral particles with diameter $2R=u_g$.

Returning to the problem of specifying the unknown compressional rigidity modulus

$$\mu_c=\frac{(\frac{4}{3}\eta_f+\lambda_f)}{t_0}\,\Gamma(1-n), \tag{38}$$

it is now assumed that μ_c is proportional to the radius, a, of the area of contact between contiguous mineral grains, as given by Eq. (37). Accordingly, the coefficient of compressional dissipation may be expressed in the form

$$\chi_f=\frac{\mu_c}{\rho_0 c_0^2}=\left(\frac{u_g}{u_0}\right)^{1/3}\frac{\mu_0}{\rho_0 c_0^2}, \tag{38′}$$

where, as in the phi units of grain size, the reference grain diameter is chosen as $u_0=1000\,\mu$m, representing very coarse sand, and $\mu_0=2\times10^9$ Pa is a constant of proportionality that has been selected on the basis of a best fit to compressional-wave speed versus grain-size data (see Fig. 8 in I). Although Eq. (38′) apparently contains two scaling parameters, u_0 and μ_0, it should be obvious that they are not independent and that there is in effect only one, namely $\mu_0/(u_0)^{1/3}=2\times10^8$ Pa/$(\mu\text{m})^{1/3}$. The formulation in Eq. (38) has been chosen to avoid a single scaling constant with the rather awkward units of pressure/(length)$^{1/3}$.

Equation (38′) states that the compressional rigidity modulus, μ_c, is proportional to the length of the line of highest tensile stress between grains. According to Hertz's result in Eq. (37), the length of this line depends on several factors apart from particle size, including the force, F, pressing the two particles together. If it were assumed that this force scales with the overburden pressure, which itself is approximately proportional to the depth of the sediment, D, then Eq. (38′) could easily be extended to give the near-interface depth dependence of μ_c, χ_f and thence of c_p. That is to say, the depth dependence of μ_c, χ_f, and c_p is contained in the coefficient μ_0, and $\mu_0\propto F^{1/3}\propto D^{1/3}$, which implies that c_p varies rather weakly with depth, consistent with the observations of Hamilton[6] and Richardson and Briggs.[24] Although the depth dependence of c_p is of considerable interest in connection with various applications, it is not pursued here. For our present purpose, we confine our attention to surficial sediments and treat μ_0 as a constant with the value given above. Then, it follows from Eq. (38′) that the functional dependence of the compressional speed on particle size is given by

$$c_p=\sqrt{c_0^2+\left(\frac{u_g}{u_0}\right)^{1/3}\frac{\mu_0}{\rho_0}}, \tag{39}$$

where c_0 and ρ_0 themselves depend on u_g through Eqs. (33), (35), and (36′).

To establish its dependence on particle size, the dissipative, shear rigidity modulus, μ_s, in Eq. (20) is treated in a similar way to μ_c in the expression for χ_f. In this case, however, we assume that μ_s is proportional to the area, πa^2, of the circle of contact between mineral grains, which gives rise to the expression

$$\mu_s = \left(\frac{u_g}{u_0}\right)^{2/3} \mu_1, \tag{40}$$

where the constant of proportionality is $\mu_1 = 5.1 \times 10^7$ Pa and, as before, $u_0 = 1000$ μm. Again, only one scaling constant is actually present in the formulation in Eq. (40), namely $\mu_1/(u_0)^{2/3} = 5.1 \times 10^5$ Pa/(μm)$^{2/3}$. It is implicit in Eqs. (37) and (40) that $\mu_s \propto F^{2/3} \propto D^{2/3}$, that is, μ_s scales as the sediment depth, D, raised to the power of 2/3. From Eq. (30), this corresponds to a shear speed, c_s, that is proportional to $D^{1/3}$, which is very close to the empirical fractional power-law depth dependencies for c_s discussed by Hamilton[40] and Richardson *et al.*[34] As with c_p, the depth dependence of c_s is not pursued here, but instead only surficial sediments are considered, as described by Eq. (40), with μ_1 taking the value stated above.

It follows from Eqs. (30) and (40) that the dependence of the shear speed on particle size is given by

$$c_s = \left(\frac{u_g}{u_0}\right)^{1/3} \sqrt{\frac{\mu_1}{\rho_0}}, \tag{41}$$

where ρ_0 is a function of u_g through Eqs. (33) and (36′).

The expressions discussed in this and the preceding section allow the wave speeds c_p and c_s, along with the associated attenuation coefficients, to be plotted as functions of any one of the mechanical properties of the sediment (i.e., particle size, density, or porosity). Only four unknown parameters appear in the theory of the mechanical properties of the sediment, three of which (Δ, μ_0, and μ_1) have been assigned non-adjustable values, which are representative of surficial sediments. The fourth parameter, γ, which appears in Eq. (36a) for the porosity, is zero for sands and many of the coarser silts but, for the finer sediments, γ should be determined from a match to porosity data.

VII. COMPARISON WITH DATA

The expressions developed above relating to compressional-wave properties have been compared in I with a number of comprehensive data sets and shown to align accurately with the measurements. The expressions for the shear properties are rather more difficult to verify because published shear data are comparatively rare. This is especially true of direct measurements of shear parameters. Indirect estimates of shear properties, for example, shear speed inferred from the measured speed of an interface wave, are unsuitable for comparison with the predictions of the new theory. However, a few direct measurements of shear parameters can be found in the literature and these are compared below with the theory.

Figures 5 to 7 show the shear speed versus mean grain size, porosity and compressional speed, for a variety of sediments ranging from very fine-grained clays to coarse sand. As identified in the legends to the figures, the data in Figs. 5–7 are from a number of papers that have been published over recent years by Richardson[23,24,34–36,41] and colleagues. For the purpose of the comparisons, the theoretical curves in Figs. 5–7 have been computed with the bimodal size parameter, γ, set to zero.

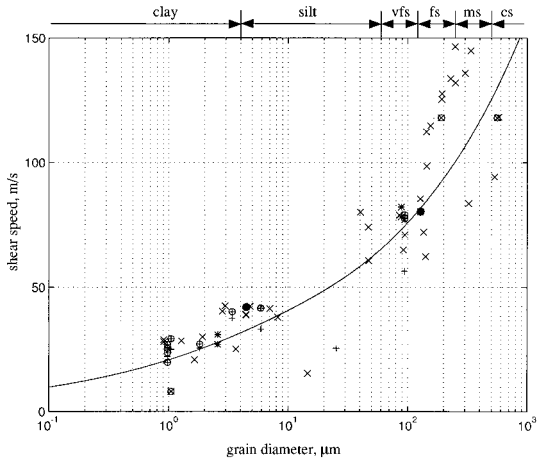

FIG. 5. Shear speed versus grain size. The solid line is the theoretical expression in Eq. (41) and the symbols represent data from the following publications: circle with plus sign (⊕), Richardson *et al.* (Ref. 23); circle with cross (⊗), Richardson and Briggs (Ref. 24); plus sign (+), Richardson *et al.* (Ref. 34), asterisk (*), Barbagaleta *et al.* (Ref. 35); cross (×), Richardson (Ref. 36); solid circle (●), Richardson (Ref. 41). The key to the sediment types is in the legend to Fig. 3.

It can be seen in Fig. 5 that the predicted shear speed follows the trend of the data fairly accurately over some three decades of particle size. Similarly, the theoretical relationship in Fig. 7, between shear speed and compressional speed, aligns quite nicely with the data. The shear speed as a function of porosity in Fig. 6 is also predicted reasonably well by the theory, although in this case the data for the higher porosity, finer sediments fall slightly below the theoretical line. This is perhaps not surprising, since these are the types of sediment that often show a bimodal particle-size distribution and a correspondingly reduced porosity. With γ set to zero, this effect has been excluded from the theoretical curve in Fig. 6, which accordingly is somewhat high.

It is evident in Figs. 3–7 that the experimental points show some spread, part of which may be attributed to experimental error and also to the fact that the various data sets were collected under very different environmental conditions. Factors such as ambient temperature, water depth, measurement depth beneath the bottom interface, sediment

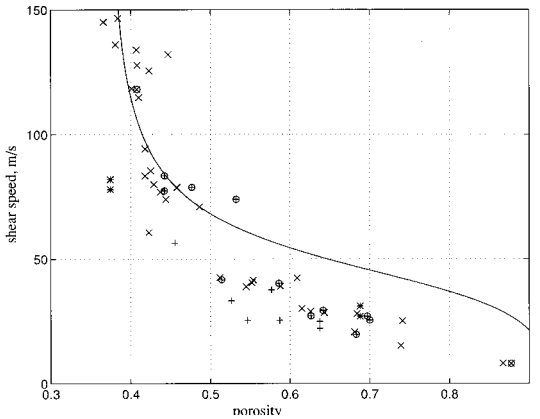

FIG. 6. Shear speed versus porosity. The solid line is the theory from Eqs. (41) and (36a) with $\gamma = 0$, and the symbols represent data, as identified in the legend to Fig. 5.

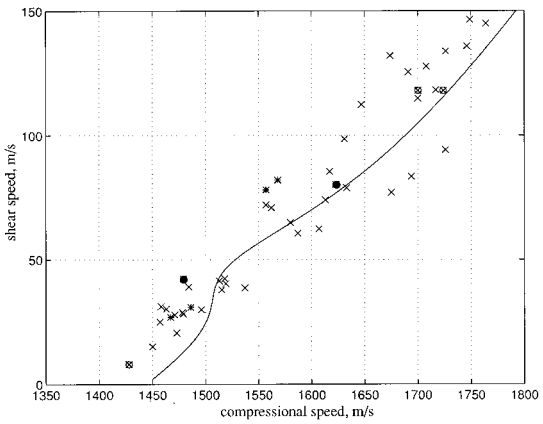

FIG. 7. Shear speed versus compressional speed. The solid line is from the theory in the text and the symbols represent data, as identified in the legend to Fig. 5.

inhomogeneity, bioturbation, and gas-bubble inclusions could all lead to variations in the observed properties of the sediment. Similarly, deviations in the bulk modulus and density of the mineral particles from the values cited above could also introduce some variability into the data. Nevertheless, the theoretical curves plotted in Figs. 5–7, as evaluated from the expressions developed here, with fixed values for all the constants, can be seen to follow the trends of the data very satisfactorily.

In fact, the good agreement between theory and experiment warrants some comment. For instance, the compressional and shear wave speeds, respectively, vary with particle size as shown in Fig. 8 in I and in Fig. 5. In both cases, the agreement between theory and data extends over about three decades of particle size, from coarse sands down to fine clays. Now, the theoretical expressions for the wave speeds have been developed principally on the basis of the Hertz theory of elastic spheres in contact, which is a reasonable model of sand grains. However, the mineral particles in clay are rather more like platelets with a very high aspect ratio, which raises the question as to why the theory should fit the data for clayey materials as well as it does?

With regard to intergranular dissipation, it seems that the mineral particles in clay interact, not individually but on average as an ensemble, as though they were ''equivalent spheres'' of volume equal to the mean volume of the particles themselves. In this sense, it could be argued, clay particles are little different from sand grains. This interpretation is consistent with the continuity in the data points in Fig. 5, for example, which appear to follow a smooth curve, exhibiting no abrupt change in behavior in the region separating clays from the coarse silts and sands. The physics of particle interactions in clays, especially in the context of wave propagation, is a subject which is still under development, so must be deferred to another time.

Perhaps the most pressing need now is the acquisition of more, directly measured, *in situ* wave properties, particularly attenuations, supplemented by mechanical data from cores. Such measurements are challenging but feasible with the advent of remotely deployed platforms like ISSAMS,[35,42] which employs bimorph ceramic bender transducers for measuring shear-wave properties directly.

VIII. ATTENUATION AND THE MATERIAL MEMORY FUNCTIONS

The small exponents n and m in the material response functions, Eqs. (6) and (7), characterize the length of the ''memory'' of the medium. A longer memory corresponds to a smaller exponent and *vice versa*. These exponents, n and m, respectively, also govern the levels of the compressional and shear attenuation in the sediment. This is evident from the expressions in Eqs. (31) and (32) for the loss tangents β_p and β_s:

$$\beta_p = \frac{n\pi}{4}\,\frac{\chi_f}{(1+\chi_f)} \tag{42}$$

and

$$\beta_s = \frac{m\pi}{4}. \tag{43}$$

According to these expressions, the attenuation in sediments is a direct manifestation of the material memory. With an indefinitely long memory (i.e., n and m vanishingly small), there would be no attenuation. Notice that β_s is independent of the particle size but β_p depends on grain size through the presence of χ_f.

It has been argued in I that the exponent of the memory function is not determined primarily by the bulk mechanical properties of the sediment (grain size, density, or porosity) but by the bonding forces between particles, which depend on the microstructure and physicochemical nature of the sediment grains. Evidence for this conclusion lies in the fact that sediments with essentially identical mechanical properties may show significantly different levels of attenuation. That is to say, there is a lack of correlation between the attenuation and the bulk properties of sediments (see Figs. 11 and 13 in I). This implies that the attenuation and hence the memory are governed by the microstructure of the medium.

Supposing this to be the case, then in a given sediment, which is assumed to be (locally) homogeneous and isotropic, it is reasonable to surmise that the compressional and shear memories are each determined by the same microscopic interactions between particles. According to this hypothesis, the two memories would have exactly the same length, that is, the exponents of the compressional and shear memory functions, n and m, respectively, would be equal.

Assuming that equality does hold between n and m, then the ratio of the compressional and shear attenuation coefficients in Eqs. (42) and (43) is independent of the memory exponents:

$$\frac{\beta_s}{\beta_p} = \frac{(1+\chi_f)}{\chi_f}, \qquad \text{for} \quad m=n. \tag{44}$$

It is evident from this expression that, with $m=n$, the shear attenuation must always be greater than the compressional attenuation. Figure 8 shows the attenuation ratio versus particle size, u_g, as evaluated using the expressions in Eqs. (44) and (38). It can be seen that the ratio in Eq. (44) decreases

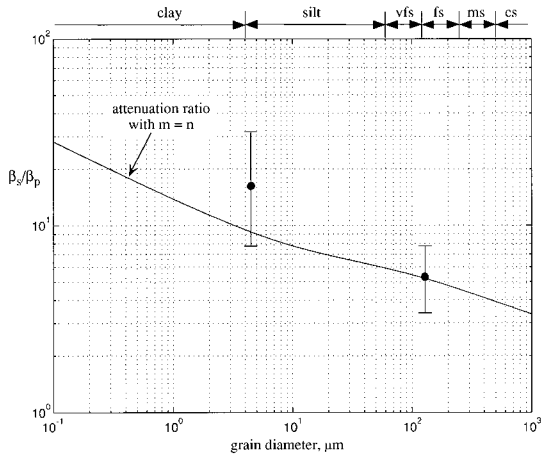

FIG. 8. Ratio of shear to compressional attenuation (loss tangents) as a function of the mean particle size. The solid line is the theory for $n=m$ from Eqs. (44) and (38a). The solid circles (●) represent the two data points from Richardson (Ref. 41), and the key to the sediment types is in the legend to Fig. 3.

monotonically with increasing particle size, from a value of 15 for clay ($u_g \approx 1\ \mu$m) to 4 for coarse sand ($u_g \approx 500\ \mu$m). This variation arises entirely from the dependence of β_p on particle size.

To test the hypothesis that $m=n$, measurements of the compressional and shear attenuation in the same sediment are required for comparison with the theoretical prediction in Fig. 8. It is emphasized, however, that these measurements must be performed on the same sediment sample. Otherwise, even with nominally similar sediments, the microscopic intergrain interactions could be quite different, which would compromise the comparison.

Measurements of the compressional and shear attenuation coefficients in the same sediment were reported recently by Richardson.[41] He investigated two types of sedimentary material from the northern California continental shelf, a fine sand, and a clayey silt, with mean particle diameters of 128 and 4.4 μm, respectively. The ratio of the measured attenuations in each of these materials is shown in Fig. 8 as the solid circles, with the error bars representing standard deviations, as reported by Richardson[41] in his Table I.

It is apparent that, within the limits of experimental error, both of Richardson's[41] data points support the hypothesis that $m=n$. For these two sediments, the numerical values of the memory exponents may be determined from Richardson's[41] shear attenuation coefficients: $\beta_s=0.0875$ (fine sand) and 0.0656 (clayey silt), corresponding to values of $m=0.11$ and $m=0.084$, respectively. Although the comparison of data with theory in Fig. 8 is consistent with the idea that the shear and compressional memory exponents are the same, it should be borne in mind that a sample population of two is hardly sufficient to reach a definitive conclusion. Whether equality between m and n is a general property of marine sediments is a question that will be resolved only as more experimental evidence on shear and compressional attenuation becomes available.

IX. CONCLUDING REMARKS

A new analysis of wave propagation in a saturated marine sediment, consisting of mobile mineral grains and seawater, has been presented above. The medium has been treated as a fluid, with an elastic rigidity modulus set identically to zero. Dissipation, associated with intergrain contacts, has been formulated to account for hysteresis in the material by introducing material memory functions with a specific functional form. These memory functions give rise to a wave equation not only for a compressional wave but also for a transverse wave, that is to say, this particular type of dissipative fluid can support the propagation of shear waves. In effect, the intergranular dissipation provides the material with a certain ''dissipative'' rigidity, even though the medium has no elastic rigidity. Such behavior is not possible in say a viscous fluid, where a transverse disturbance is critically damped and does not propagate as a true wave.

One of the interesting predictions of the new theory is an attenuation coefficient for both the compressional and shear wave that is proportional to the first power of frequency. Fairly compelling experimental evidence[15] indicates that this type of frequency dependence is exhibited by the attenuation coefficient of compressional waves in sediments. The data on attenuation of shear waves in sediments are more limited, but a linear dependence on frequency has been observed,[17,18] under laboratory conditions, in water-saturated sands and unconsolidated glass beads.

In I, a model of the mechanical properties of a sediment was introduced, which has been combined here with the wave analysis to obtain expressions relating the compressional and shear-wave speeds to the grain size, porosity, and density of the medium. Comparisons of these expressions with published data, for a variety of sediments ranging from clays to coarse sand, show that the theory follows the trend of the measurements reasonably accurately. Thus by specifying the grain size, for example, the theory yields sensible estimates of the compressional and shear speeds, the density and the porosity.

If certain dissipative, fluidlike (zero elastic rigidity modulus) sediments can support shear, they should also be capable of supporting an interface wave at the water–sediment boundary, the theoretical properties of which have yet to be established. Such a development would be relevant to a number of applications, where interface waves are used as tools for investigating the properties of ocean sediments.[3,43]

ACKNOWLEDGMENTS

Dr. Michael Richardson very kindly provided me with a preprint (Ref. 41) containing his most recent compressional and shear attenuation data, which have been reproduced here in Fig. 8. This research was supported by the Office of Naval Research under Grant No. N00014-91-J-1118, which is appreciated.

[1] M. J. Buckingham, ''Theory of acoustic attenuation, dispersion and pulse propagation in granular materials including marine sediments,'' J. Acoust. Soc. Am. **102**, 2579–2596 (1997).

[2] J. M. Hovem, M. D. Richardson, and R. D. Stoll (Eds.), *Shear Waves in Marine Sediments* (Kluwer, Dordrecht, 1991).
[3] E. L. Hamilton, H. P. Bucker, D. L. Keir, and J. A. Whitney, ''Velocities of compressional and shear waves in marine sediments determined in situ from a research submersible,'' J. Geophys. Res. **75**, 4039–4049 (1970).
[4] E. L. Hamilton, ''Elastic properties of marine sediments,'' J. Geophys. Res. **76**, 579–604 (1971).
[5] K. B. Briggs, ''Comparison of measured compressional and shear wave velocity values with predictions from Biot theory,'' in *Shear Waves in Marine Sediments*, edited by J. M. Hovem, M. D. Richardson, and R. D. Stoll (Kluwer, Dordrecht, 1991), pp. 121–130.
[6] E. L. Hamilton, ''V_p/V_s and Poisson's ratios in marine sediments and rocks,'' J. Acoust. Soc. Am. **66**, 1093–1101 (1979).
[7] A. R. Gregory, ''Fluid saturation effects on dynamic elastic properties of sedimentary rocks,'' Geophysics **41**, 895–921 (1976).
[8] M. A. Biot, ''Theory of propagation of elastic waves in a fluid-saturated porous solid: I. Low-frequency range,'' J. Acoust. Soc. Am. **28**, 168–178 (1956).
[9] M. A. Biot, ''Theory of propagation of elastic waves in a fluid-saturated porous solid: II. Higher frequency range,'' J. Acoust. Soc. Am. **28**, 179–191 (1956).
[10] M. A. Biot, ''Mechanics of deformation and acoustic propagation in porous media,'' J. Appl. Phys. **33**, 1482–1498 (1962).
[11] M. A. Biot, ''Generalized theory of acoustic propagation in porous dissipative media,'' J. Acoust. Soc. Am. **34**, 1254–1264 (1962).
[12] T. J. Plona, ''Observation of a second bulk compressional wave in a porous medium at ultrasonic frequencies,'' Appl. Phys. Lett. **36**, 259–261 (1980).
[13] D. L. Johnson and T. J. Plona, ''Acoustic slow waves and the consolidation transition,'' J. Acoust. Soc. Am. **72**, 556–565 (1982).
[14] P. M. Morse and H. Feshbach, *Methods of Theoretical Physics: Part I*, International Series in Pure and Applied Physics (McGraw-Hill, New York, 1953).
[15] E. L. Hamilton, ''Compressional-wave attenuation in marine sediments,'' Geophysics **37**, 620–646 (1972).
[16] E. L. Hamilton, ''Acoustic properties of sediments,'' in *Acoustic and the Ocean Bottom*, edited by A. Lara-Saenz, C. Ranz Cuierra, and C. Carbo-Fité (Consejo Superior de Investigacions Cientificas, Madrid, 1987), pp. 3–58.
[17] B. A. Brunson and R. K. Johnson, ''Laboratory measurements of shear wave attenuation in saturated sand,'' J. Acoust. Soc. Am. **68**, 1371–1375 (1980).
[18] B. A. Brunson, ''Shear wave attenuation in unconsolidated laboratory sediments,'' in *Shear Waves in Marine Sediments*, edited by J. M. Hovem, M. D. Richardson, and R. D. Stoll (Kluwer, Dordrecht, 1991), pp. 141–147.
[19] J. W. S. Baron Rayleigh, *The Theory of Sound I* (Dover, New York, 1945).
[20] J. W. S. Baron Rayleigh, *The Theory of Sound II* (Dover, New York, 1945).
[21] K. F. Graff, *Wave Motion in Elastic Solids* (Dover, New York, 1975).
[22] A. Erdélyi (Ed.) *Tables of Integral Transforms, Volume 1*, Bateman Manuscript Project (McGraw-Hill, New York, 1954).
[23] M. D. Richardson, E. Muzi, L. Troiano, and B. Miaschi, '' Sediment shear waves: A comparison of *in situ* and laboratory measurements,'' in *Microstructure of Fine-Grained Sediments*, edited by R. H. Bennett, W. R. Bryant, and M. H. Hulbert (Springer-Verlag, New York, 1991), pp. 403–415.
[24] M. D. Richardson and K. B. Briggs, ''*In situ* and laboratory geoacoustic measurements in soft mud and hard-packed sand sediments: Implications for high-frequency acoustic propagation and scattering,'' Geo-Marine Lett. **16**, 196–203 (1996).
[25] R. Kronig, ''On the theory of dispersion of x-rays,'' J. Opt. Soc. Am. **12**, 547–557 (1926).
[26] H. A. Kramers, ''La diffusion de la lumiere par les atomes,'' Atti Congr. Intern. Fisica, Como 2, 545–557 (1927).
[27] M. O'Donnell, E. T. Jaynes, and J. G. Miller, ''Kramers-Kronig relationship between ultrasonic attenuation and phase velocity,'' J. Acoust. Soc. Am. **69**, 696–701 (1981).
[28] A. B. Wood, *A Textbook of Sound* (G. Bell, London, 1964).
[29] J. C. Molis and N. P. Chotiros, ''A measurement of the grain bulk modulus of sands,'' J. Acoust. Soc. Am. **91**, 2463(A) (1992).
[30] N. P. Chotiros, ''Biot model of sound propagation in water-saturated sand,'' J. Acoust. Soc. Am. **97**, 199–214 (1995).
[31] R. D. Stoll, *Sediment Acoustics* (Springer-Verlag, Berlin, 1989).
[32] O. K. Rice, ''On the statistical mechanics of liquids, and the gas of hard elastic spheres,'' J. Chem. Phys. **12**, 1–18 (1944).
[33] E. L. Hamilton, ''Sound velocity and related properties of marine sediments, North Pacific,'' J. Geophys. Res. **75**, 4423–4446 (1970).
[34] M. D. Richardson, E. Muzi, B. Miashi, and F. Turgutcan, ''Shear wave velocity gradients in near-surface marine sediment,'' in *Shear Waves in Marine Sediments*, edited by M. Hovem, M. D. Richardson, and R. D. Stoll (Kluwer, Dordrecht, 1991), pp. 295–304.
[35] A. Barbagelata, M. D. Richardson, B. Miashi, E. Muzi, P. Guerrini, L. Troiano, and T. Akal, ''ISSAMS: An *in situ* sediment acoustic measurement system,'' in *Shear Waves in Marine Sediments*, edited by J. M. Hovem, M. D. Richardson, and R. D. Stoll (Kluwer, Dordrecht, 1991), pp. 305–312.
[36] M. D. Richardson, ''*In situ* shallow-water sediment geoacoustic properties,'' in *Shallow Water Acoustics*, edited by J. X. Zhou (Institute of Acoustics, Beijing, 1997).
[37] M. D. Richardson and K. B. Briggs, ''On the use of acoustic impedance values to determine sediment properties,'' Proc. Inst. Acoust. **15**, 15–24 (1993).
[38] M. D. Richardson, ''Spatial variability of surficial shallow water sediment geoacoustic properties,'' in *Ocean-Seismo Acoustics: Low-Frequency Underwater Acoustics*, edited by T. Akal and J. M. Berkson (Plenum, New York, 1986), pp. 527–536.
[39] S. P. Timoshenko and J. N. Goodier, *Theory of Elasticity* (McGraw-Hill, New York, 1951).
[40] E. L. Hamilton, ''Shear-wave velocity versus depth in marine sediments: A review,'' Geophysics **41**, 985–996 (1976).
[41] M. D. Richardson, ''Attenuation of shear waves in near-surface sediments,'' in *High Frequency Acoustics in Shallow Water*, edited by N. G. Pace (NATO SACLANT Undersea Research Centre, La Spezia, 1997), pp. 451–458.
[42] S. R. Griffin, F. B. Grosz, and M. D. Richardson, ''*In situ* sediment geoacoustic measurement system,'' Sea Technol. 19–22 (1996).
[43] G. Nolet and L. M. Dorman, ''Waveform analysis of Scholte modes in ocean sediment layers,'' Geophys. J. Int. **125**, 385–396 (1996).